Headline Articles

Structure of Clusters in Ethanol–Water Binary Solutions Studied by Mass Spectrometry and X-Ray Diffraction

Masaki Matsumoto, Nobuyuki Nishi,* Toshiya Furusawa,† Masaru Saita,† Toshiyuki Takamuku,†† Motoyuki Yamagami,††† and Toshio Yamaguchi,†††

Department of Chemistry, Faculty of Science, Kyushu University, Hakozaki, Fukuoka 812-81

†Suntory Research Center, Wakayawadai 1-1-1, Shimamoto-cho, Mishima-gun, Osaka 618

††Research & Development Div., TOTO Ltd., Nakashima, Kokurakita-ku, Kitakyushu 802

†††Department of Chemistry, Faculty of Science, Fukuoka University, Nanakuma, Fukuoka 814-80

(Received February 13, 1995)

The structure of clusters in ethanol–water binary solutions at x_E (ethanol mole fraction) ≥ 0.2 was investigated by the mass-spectrometric analysis of clusters isolated from liquid droplets and X-ray diffraction measurements of the intact solution. The average number of water molecules (N^a) of the ethanol m-mer hydrates ($5<m<15$) in the mixtures at $0.2\leq x_E\leq 0.8$ was found to be expressed by a function of the water mole fraction (x_w), $N^a=\{(m/4.2)-1\}^2$ ($x_w+0.85$), suggesting that the fundamental structure of ethanol polymer-hydrates is invariable in this region. An inflection point of N^a was found at $x_E\approx 0.2$. The radial distribution functions (RDFs) from X-ray measurements demonstrated a decrease of linear hydrogen bonds at 2.8 Å with increasing x_E, while keeping the strongest peak at 4.8 Å for $0.4\leq x_E\leq 1.0$. On the basis of a composition analysis of the mass spectra and the concentration dependence of RDFs, we propose the most likely model of ethanol–water binary clusters formed in the region $0.2\leq x_E\leq 0.8$.

Ethanol–water mixtures are often used as solvents in studies of chemical equilibria and reactions as well as the protein extraction from various biological tissues. The partial molar volumes and thermochemical properties of alcohol–water mixtures have been precisely investigated.[1—3] Studies carried out before 1966 were reviewed by Franks and Ives.[4] From a theoretical point of view, Ben-Naim presented a new procedure which provides information concerning the affinity between two species in a mixture of two components.[5] The application of this procedure to an ethanol–water system produced a very interesting behavior for the quantity G_{AW}, which is defined as an integral over the pair correlation function between ethanol and water molecules. This quantity conveys the average affinity of alcohol to water molecules. The derived G_{AW} showed a very steep decrease with increasing alcohol in aqueous media; its minimum appeared at x_E (ethanol mole fraction)=0.04. On the other hand, he also found that the quantity G_{AA} (average affinity between alcohol molecules) attains a maximum at $x_E=0.1$. This was attributed to an enhancement in the strength of the hydrophobic interaction.

The chemical shifts in NMR measurements provide information on hydrogen bonding in an ethanol–water mixture.[6] Coccia et al. performed a comprehensive study, finding that the ethanol–water interaction seen based on different line shapes of the hydroxyl signals changed depending on the ethanol concentration.[7] The chemical shift to a lower field was attributed to an enhanced interaction of water with the ethanol alkyl group. They concluded that the "structure-making" effect, occurring in the range $0<x_E<0.08$, is accompanied by a corresponding increase in the self-association of water molecules. For the region $0.08<x_E<0.20$ they suggested that the ethanol ethyl groups, becoming more and more numerous, begin to prevent water from organizing into three-dimensional structures, so that the "structure-making" power becomes progressively less effective. The changes of the OH chemical shift and the line shape indicated that the structural behavior of these solutions is strongly modified at $x_E>0.2$. They suggested, based on the chemical shifts of the hydroxyl protons, that the behavior of water–alcohol mix-

tures cannot be considered in terms of a single molecular mechanism over the entire concentration range. The total concentration range was divided into four regions, distinguished above all by different line shapes of the hydroxyl signals: (i) $0.00 \leq x_E \leq 0.08$; (ii) $0.08 \leq x_E \leq 0.20$; (iii) $0.20 \leq x_E \leq 0.80$; (iv) $0.80 \leq x_E \leq 1.00$. In region (iii), a large number of ethanol–water bonds are formed, while the water–water bonds are broken.

Mashimo et al. reported that a $\log \tau$ plot against x_E cannot be explained by a single straight line, but by two straight lines, where τ is the relaxation time in the dielectric measurement.[8] They noted that the point of intersection of these two lines is $x_E = 0.17$, and mentioned that chain-like clusters are undoubtedly generated in the region $0 < x_E < 0.18$.

The structure of water and alchols was investigated by X-ray and neutron diffraction measurements.[9—15] Narten and Habenschuss[16] showed that hydrogen bonded hydroxyl groups appear in methanol and ethanol with an OH–OH distance of 2.8 Å, and that each hydroxyl group has 1.8±0.1 nearest neighbors. They mentioned that the result could be understood in terms of chain formation, and that the molecules within such a chain are connected by OH–OH hydrogen bonds. Nishikawa and Iijima reported based on small-angle X-ray scattering that in aqueous ethanol solutions there are no large clusters which give a prominently different electron density or neutron-scattering power from that of the surrounding.[17]

We have reported on a study of hydrogen-bonding cluster formation of ethanol and water molecules in diluted aqueous solutions ($x_E \leq 0.3$).[18] The structure function at $x_E = 0.02$, obtained from an X-ray diffraction measurement, showed a striking resemblance to the pure water curve at 1000 bar. The radial distribution function exhibited a decrease of linear hydrogen bonds at 2.8 Å, and new peaks appeared at 3.3 and 3.8 Å with increasing x_E. The peak at 3.8 Å was assigned to the C···O distance between one of the carbon atoms of ethanol and the oxygen atom of a cage water. The mass spectra of the clusters isolated from the same solution at 35 °C suggested that the stacking of ethyl groups already occurs even at this concentration. All of these results have led to a cluster model of a stacked ethanol core and a thin water shell (or mantle). Motional activity of such large shell-type clusters was thought to cause a breakdown of the bulk water structure. These observations for a diluted aqueous solution of ethanol suggested the evolution of an ethanol polymer structure and complete break down of the bulk water structure at $x_E > 0.1$.

We also investigated the molecular association in ethanol–water mixtures by a mass-spectrometric analysis of isolated clusters; our results have showed that the ethanol–ethanol interaction is nearly the same as that of the water–water pairs based on ab intio molecular orbital calculations.[18,19] Although the previous work was limited to the region of mass numbers ≤ 360, we found mass spectral changes characteristic of the ethanol concentrations. One of the most important results is that the presence of water is a key function for the formation of large ethanol polymers. Here, we report on a more quantitative analysis of the mass spectra and the X-ray diffraction measurement in the $0.18 \leq x_E \leq 1.00$ region.

Experimental

Mass Spectrometric Study. The apparatus and experimental details for generating cluster beams from a liquid were essentially the same as those reported before.[20,21] Aqueous ethanol solutions were converted to mist particles in the first and second expansion chambers. The first skimmer was situated 2 mm downstream from a needle nozzle; the second skimmer was located at 8 mm further downstream. A flow rate of 0.09 $cm^3\,min^{-1}$ was adopted. After passing the second skimmer the mist particles in the beam showed an adiabatic explosion to clusters and free molecules. The vacuum of the ionization region was maintained below 1.3×10^{-4} Pa. The clusters were ionized by 40 eV electron impact and analyzed by a quadrupole mass spectrometer (Extrel 7-162-8+311-12H) with an axial ionizer (Extrel 041-3). The clusters produced in the region of an ionizer are most effectively analyzed by the mass spectrometer. Signals from a ceramic electron multiplier (Murata EMS-6081B) were accumulated typically for 60 sweeps using a Nicolet 1170 signal averager.

The temperature of the liquid droplets was estimated by measuring the mass spectral change of an aqueous solution of propionic acid with $x_E = 0.005$, the temperature dependence of which had been calibrated by measuring the lower and upper critical temperatures (49 and 129 °C, respectively) of a 5% aqueous solution of 2-buthoxyethanol. The average temperature of the liquid droplets was 35 °C.

Ethanol of high-performance liquid-chromatography grade (Wako Pure Chemicals, 99.5%) was used without further purification, and high purity water was prepared by using a PuricZ water purifer (Organo Co.).

X-Ray Diffraction Measurements. All X-ray diffraction measurements were carried out at room temperature with a rapid X-ray diffractometer using an imaging plate (IP) (DIP301, MAC Science Co., Ltd.), which was newly developed for the X-ray diffraction of liquid and amorphous samples. Details concerning this apparatus and performance have been described elsewhere.[22,23] X-Rays were generated at a rotary Mo anode operated at 50 kV and 200 mA, and then monochromatized by a graphite crystal to obtain Mo $K\alpha$ radiation ($\lambda = 0.7107$ Å). The sample solution sealed in a glass capillary (1 mmϕ) was exposed to X-rays. The observed range of the scattering angle (2θ) was from 2° to 140°, corresponding to a scattering vector ($s = 4\pi \sin\theta/\lambda$) of 0.3 to 16 $Å^{-1}$. The exposure time was three hours for the measurement of one sample.

The measured two-dimensional intensity data ($I_{obsd}(x,y)$) on IP were integrated into one dimentional data ($I_{obsd}(\theta)$) as previously reported.[22,23] Corrections were made for the background,[23] adsorption,[23] polarization,[24] and multiple scattering[24] of X-rays to the observed intensities. The structure functions ($i(s)$) are given by

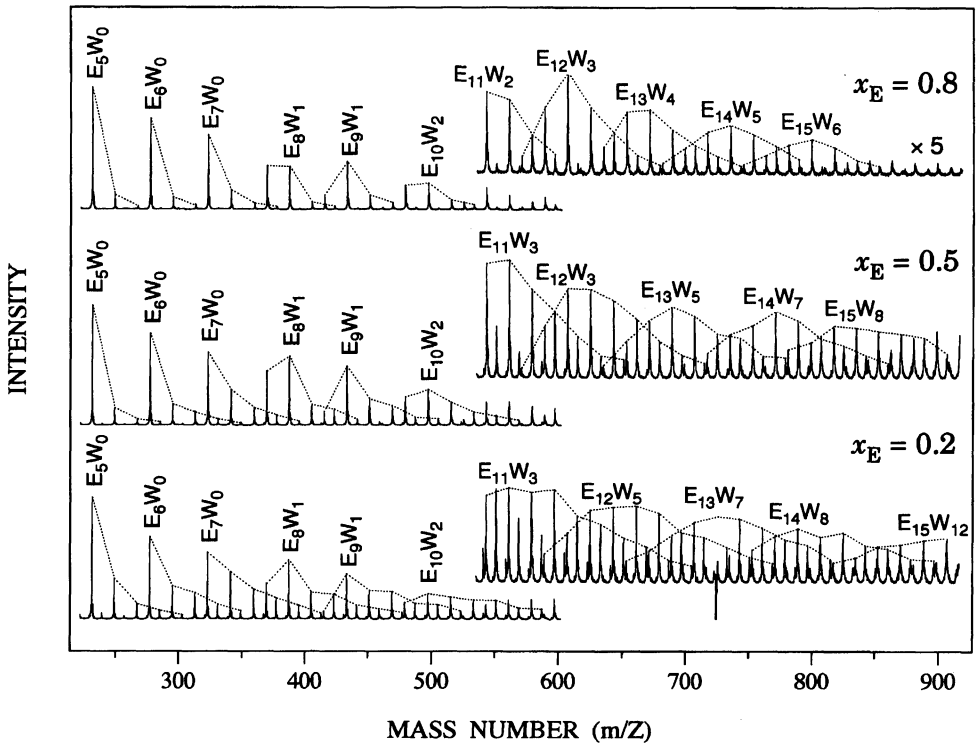

Fig. 1. Mass spectra of the clusters isolated from ethanol–water binary solutions with x_E=0.8, 0.5, and 0.2. Average droplet temperature is estimated to be 35 °C.

$$i(s) = KI(s) - \sum_j n_j f_j^2(s), \quad (1)$$

where K represents a normalization factor of the observed intensities ($I(s)$) to absolute units, n_j is the number of atom j in a stoichiometric volume (V) containing one O atom, and $f_j(s)$ is the atomic scattering factor of atom j corrected for the anomalous dispersion. The scattering factors for neutral atoms were taken from the International Tables for X-ray Crystallography.[25] The $si(s)$ values are Fourier transformed into the radical distribution function ($D(r)$) as

$$D(r) = 4\pi r^2\rho_0 + (2r/\pi)\int_0^{s_{max}} si(s)M(s)\sin(rs)\,ds. \quad (2)$$

Here, ρ_0 ($=[\Sigma n_j f_j(0)]^2/V$) stands for the average scattering density of the sample solution and s_{max} is the maximum s value attained in the measurements (s_{max}=15.0 Å^{-1}). The modification function $M(s)$ has the form:

$$M(s) = \left[\sum n_j f_j^2(0)/\sum n_j f_j^2(s)\right]\exp(-k\,s)^2, \quad (3)$$

with the damping factor (k) being chosen as 0.01 Å^2 in the present case.[26] The program KURVLR[24] was used for all calculations of the X-ray data.

Results

Mass Spectrometry. Figure 1 shows the mass spectra of the clusters generated from ethanol-water binary solutions with x_E=0.8, 0.5, and 0.2 (bottom). The liquid droplet temperature was 35 °C. The mass spectra were obtained at an electron impact energy of 40 eV. The electron impact ionization evaporates some of the free water (W), or ethanol (E), and an OH radical from an binary cluster:

$$E_mW_n + e^- \rightarrow H^+E_mW_{n'} + OH + (n - n' - 1)W + 2e^- \quad (4)$$

or

$$\rightarrow H^+E_{m'}W_n + OH + (m - m' - 1)E + 2e^-. \quad (5)$$

Stace and Shukla reported that the proton is preferentially attached to an ethanol molecule.[27] Thus, the observed ionic species in Fig. 1 are the fragments (or strongly bound parts) of the original clusters. In the mass region lower than 360, the main signals are pure ethanol clusters, H^+E_m ($m<8$), while for $m\geq 8$, the intensities of the pure solute clusters become weaker relative to those of the corresponding mono-hydrate species of $H^+E_nW_1$; the hydrate clusters are thus the main species. Although the mass spectra showed moderate changes with increasing x_E, the hydration number (n) of the strongest signal in the hydration sequence of $H^+E_{11}W_n$ shifted from 2 at x_E=0.8 to 3 at x_E=0.5—0.2, even though the water-to-ethanol ratio at x_E=0.2 is 16 times larger than that at x_E=0.8. In the higher mass region of Fig. 1, where the intensity-enhanced spectra are displayed, the signals of pure ethanol clusters are very weak, even for a sample solution with x_E=0.8. The hydration number of the strongest signal (n_{max}) in an ethanol m-mer hydration sequence increases more eminently than that in the low mass spectra. For example, the value of n_{max} in the $H^+E_{13}W_n$ sequence shifted from 4 to 5, and further to 7 at x_E=0.8, 0.5, and 0.2,

respectively. However, this increase of n_{max} is rather insensitive to the increase in the molar fraction of water in the $0.2 \leq x_E \leq 0.8$ region.

In contrast to the quite moderate spectral change, the signal intensities varied sensitively to the change in x_E. Figure 2 shows the integrated intensities of m-mer hydrate ions plotted on a logarithmic scale as a function of the ethanol polymer size (m; $10 \leq m \leq 16$). The integrated intensity for a hydration sequence of each ethanol m-mer was obtained by summing up the intensities of the m-mer hydrate signals over the observable hydration numbers (n). Among the various mixtures of ethanol and water in the $0.05 \leq x_E \leq 0.67$ range, the mixture at $x_E = 0.15$ showed the most abundant hydrate clusters for $m < 12$, but the hydrate clusters with $m \geq 12$ became more abundant at $x_E = 0.18$. A further increase of the ethanol concentration resulted in a drastic decrease of the hydrates with lower polymer cores ($m < 12$) and also reduced the signals of the higher polymer-hydrates ($m \geq 12$). For example the integrated intensities of the ethanol 10-mer and 11-mer hydrates in the $x_E = 0.5$ mixture were 2 orders of magnitude weaker than those of the $x_E = 0.15$ mixture, although the intensity ratios of the higher polymer-hydrates ($m \geq 12$) of the $x_E = 0.5$ mixture to those of the $x_E = 0.15$ mixture became relatively smaller with increasing m. The hydrate signals of the $x_E = 0.67$ mixture was an order of magnitude weaker than those of the $x_E = 0.5$ mixture. This result again demonstrates that a certain number of water molecules is indispensable for stabilizing large ethanol polymers.

In order to attempt a more quantitative discussion, the Poisson distribution function was applied for a population analysis of each hydration sequence in the mass spectra. This function is a frequency distribution that is often used when the probability of each event which occurs is extremely small. Suppose that in a large number (t) of trials the probability of an event occuring is s, where s is small, but that the average number of events (λ) in any given set of t trials, namely $\lambda = ts$, is a finite number. The probability ($p(x)$) of x events occurring is

$$p(x) = e^{-\lambda} \cdot \lambda^x / x!. \quad (6)$$

The standard deviation (σ) of the distribution is given by

$$\sigma = \sqrt{\lambda}. \quad (7)$$

In the present system x corresponds to the hydration

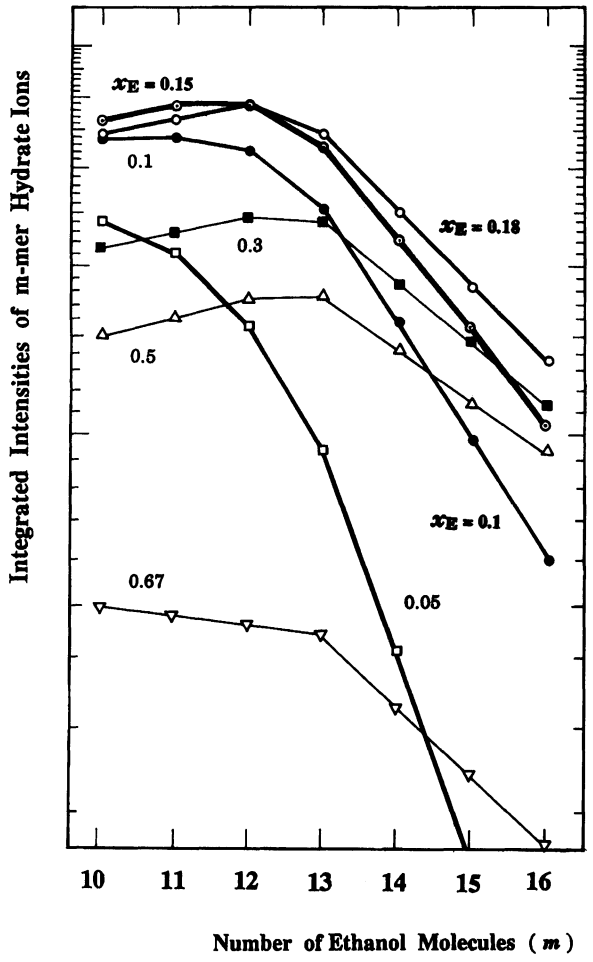

Fig. 2. Relative integrated intensities of ethanol m-mer-hydrate clusters as functions of ethanol polymer size (m; $10 \leq m \leq 16$).

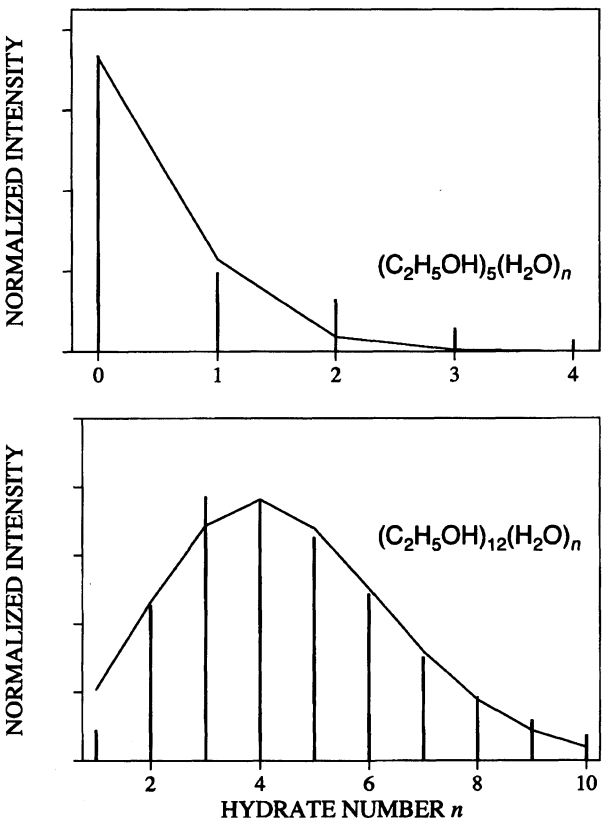

Fig. 3. Normalized distribution of ionized clusters as functions of hydration numbers (n) observed for the $x_E = 0.5$ solution. Solid lines are Poisson distribution functions. Top: E_5W_n hydration series. Bottom: $E_{12}W_n$ hydration series.

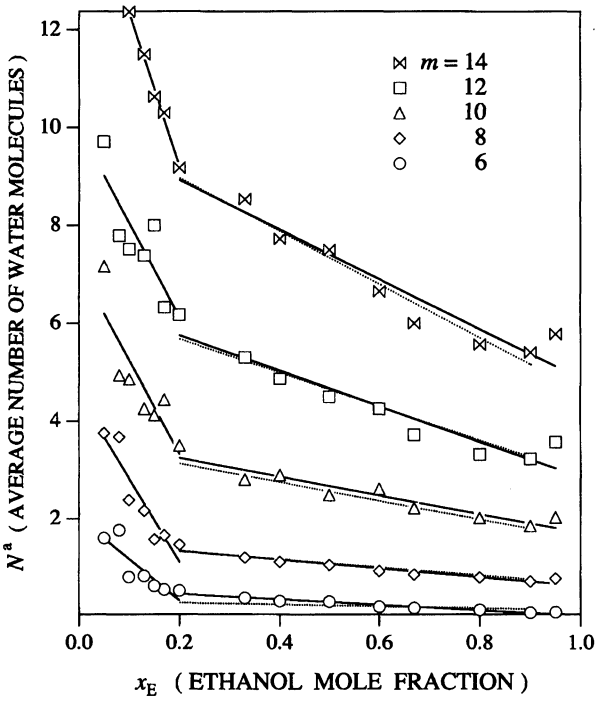

Fig. 4. Plots of average water numbers (N^a) as functions of x_E for ethanol m-mer hydrates with $m=6$, 8, 10, 12, 14. The dotted lines are obtained by using Eq. 8 for the respective m values.

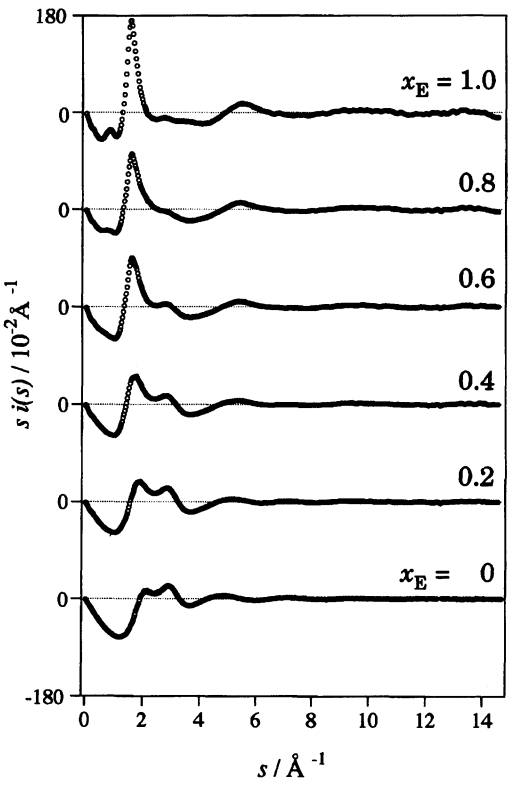

Fig. 5. Structure functions ($i(s)$) multiplied by s of ethanol–water solutions with $x_E=0$, 0.2, 0.4, 0.6, 0.8, and 1.0 at room temperature.

number (n). The intensity distribution of the hydration sequences of the respective ethanol polymers was approximated by Eq. 6 for estimating the average number of associated waters. The upper part of Fig. 3 shows an example in which the hydration number distribution of $H^+E_5W_n$ clusters observed for a solution with $x_E=0.5$ was approximated by the Poisson distribution function with $\lambda=0.31$. The distribution of a $H^+E_{12}W_n$ hydration sequence in the same spectrum was also fitted to the Poisson function with $\lambda=4.4$, as shown in the lower part of Fig. 3. Here, the obtained λ values provide average water numbers (N^a) of ethanol polymer-hydrates, $\lambda=N^a$.

Figure 4 shows the N^a values of the respective ethanol polymer-hydrates plotted as a function of x_E. The N^a value in the clusters linearly decreases with increasing x_E from 0.2 to 0.9, while at $x_E<0.2$ the average water numbers change drastically. At $x_E\geq0.2$, the slope of the plots varies rather moderately with increasing x_E. In the case of $m=12$, N^a changes from 6.2 for $x_E=0.2$ to 3.3 for $x_E=0.8$, although the water content in the former solution is 16 times more abundant than that in the latter solution. The change of N^a is very small compared to the decreasing amount of water in the original solution. The observed average hydration numbers (N^a) in the $0.2\leq x_E\leq0.8$ region is surprisingly well reproduced by the following equation:

$$N^a \approx \{(m/4.2)-1\}^2(x_w+0.85), \quad (8)$$

where x_w is the mole fraction of water in the mixture ($x_w=1-x_E$). The dotted lines shown in Fig. 4 were calculated using Eq. 8.

Table 1. Compositions of the Sample Solutions Used for the X-Ray Measurements (mol dm^{-3}). x_E : ethanol mole fraction, V: stoichiometric volume (Å^3) per oxygen atom, μ : linear absorption coefficient (cm^{-1}), ρ : density (g cm^{-3}).

x_E	C	O	H	V	ρ	μ
1.0	34.08	17.04	102.2	97.4	0.785	0.625
0.8	32.04	20.02	104.1	82.9	0.810	0.699
0.6	28.92	24.10	106.0	68.9	0.840	0.763
0.4	24.10	30.09	108.3	55.2	0.880	0.853
0.2	15.80	39.54	110.6	42.0	0.934	0.989

These results suggest that the essential cluster structure in the solutions is maintained in the $0.2\leq x_E\leq0.8$ region, despite a change in the mixing ratio. The appearance of an inflection point at $x_E=0.2$ is in good agreement with the mixing ratio dependence of the NMR chemical shift,[7] dielectric constants,[8] and change in the partial molar volume of ethanol.[4] This fact shows that the hydration behavior observed in the mass spectra reflects that in the original solution.

X-Ray Measurement. The structure functions ($i(s)$) multiplied by s for sample solutions with $x_E=1.0$, 0.8, 0.6, 0.4, 0.2, and 0 are shown in Fig. 5. The atomic compositions and densities of the sample solutions are given in Table 1. The total radial distribution func-

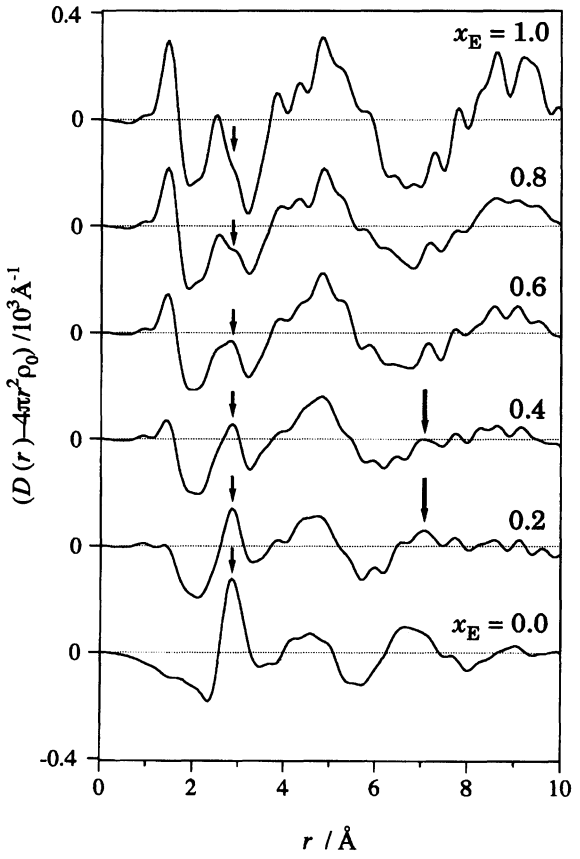

Fig. 6. Radial distribution functions in the form of $D(r)-4\pi r^2\rho_0$ of the ethanol–water binary solutions. Short arrows show the peaks at 2.8 Å assigned to the hydrogen bond distance, and long arrows indicate the peaks at 7.0 Å.

tions (RDFs) in the form of $D(r)-4\pi r^2\rho_0$ are shown in Fig. 6. In all of the RDFs, the four prominent peaks are observed at 1.5, 2.5, 2.8, and 4.8 Å. The peaks at 7—10 Å, which originate from various long-range interactions in the solutions, may suffer from overlapping spurious ripples. Thus, the peaks at $r>7$ Å were not analyzed in this work. The first peak was assigned to the intramolecular C–O and C–C distances of ethanol based on the previous X-ray[16] and neutron diffraction studies.[28] The second peak at 2.5 Å corresponds mainly to the distance between the carbon in the methyl group and the oxygen of the same ethanol molecule. This peak gradually decreases with decreasing x_E. The third peak at 2.8 Å is assigned to the hydrogen-bonded O–O distance of water–water, water–ethanol, and ethanol–ethanol pairs. The intensity of this peak grows with decreasing x_E. In particular, this peak drastically decreases in the concentration change from $x_E=0.8$ to 1.0. This indicates that the presence of 20% water molecules produces an appreciable number of hydrogen-bonds. The peak at 4.8 Å is assigned to the distance between the two carbons of the methyl–methyl and methylene–methylene pairs of the neighboring ethyl-groups, as described in the last part of Discussion.

Discussion

The appearance of an inflection point at $x_E\approx0.2$ in Fig. 4 indicates that a structural change in the mixture occurs at this concentration. On the basis of the changes of the OH chemical shift and the line shape, Coccia et al. stated that the structural behavior of ethanol aqueous solutions is quite strongly modified when the ethanol molar fraction increases above 0.2.[7] Mashimo and Umehara found that the behavior of the dielectric relaxation time also shows an inflection point at $x_E\approx0.2$.[8] They suggested that at $x_E\geq0.17$ water molecules cannot form the pure six-membered ring structure seen in ice. As reported in our previous work,[19] however, pure water clusters were not seen in the mass spectra of mixtures with $x_E>0.03$. Ethanol molecule(s) tend to attract water molecules to form an ethanol core surrounded by a water shell.[18] In order to maintain the water shell structure, the binary solution should contain a sufficient number of water molecules that can form shells as well as the bulk medium. We have reported the appearance of the 3.8 Å peak in the RDF for the solution at $x_E=0.02$.[18] This peak was attributed to the carbon–oxygen distance between a carbon atom of ethanol and an oxygen atom of shell water. The intensity of this peak became weaker with increasing ethanol concentration, showing the weakest value at $x_E=0.08$, and again gradually growing at $x_E>0.1$. Pure ethanol also showed a clear peak at 3.8 Å, as can be seen in Fig. 6. This peak is probably due to the oxygen–carbon distance of the hydrogen-bonded ethanol molecules. By fixing the hydrogen-bond distance at 2.8 Å, one can obtain a nearest oxygen–carbon distance of 3.6 Å for the hydrogen-bonded ethanols. One can therefore assign the 3.8 Å peak found in a solution with $x_E\geq0.1$ to the shortest carbon–oxygen distance of the neighboring ethanol pairs with broken (or angular) hydrogen-bonds.

The structure of the ethanol polymer-hydrates ($E_mW_n : m>8$) can be constructed based on the X-ray diffraction and the mass spectrometric data. A mass spectrometric study, however, requires careful thought for any discussion concerning the clustering structure of molecules in solution. The mass spectra provide only information about the molecular composition and intensity distribution of the ionized clusters which originate from the binding conditions of the original clusters in solution. Upon ionization, the structure of the original clusters experiences dynamical changes due to the creation of the charge. In the case of the hydrogen bonding system studied here, however, the high-mass clusters (which are large enough to dissociate a small number of weakly bound light molecules) may show slight compositional changes upon ionization. This point is easily examined by observing the drastic changes in the intensity distributions upon slight changes of the droplet temperature and size of solute molecules in addition to

the negligible changes of the mass spectra with increasing ionization energy.[20] Our analyses of the mass spectra are therefore based on an important basic assumption that the memory of the molecular composition and distribution of the original clusters is safely left in the observed distribution (or spectral feature) of the ionized clusters. If this assumption is broken, the observed mass spectra never agree with any observation of the bulk solution properties. The size-dependence study of the alkyl group on the *hydrophobic hydration* and the *hydrophobic interaction* of the carboxylic acids (which cannot be seen in the gas phase) clearly demonstrated that the mass spectrometry can provide structural information concerning clusters in an aqueous solution.[29]

From the mass spectral behavior shown in Fig. 1, the structure of ethanol–water binary clusters at $x_E > 0.2$ may be classified into two types. One is seen for clusters with ethanol molecules less than 8, which were detected as pure ethanol clusters in the mass spectra. The other one is for the clusters with more than 11 ethanol molecules accompanied by more water molecules with increasing ethanol number. Although the former is also produced by the fragmentation of larger clusters, pure ethanol polymers are thought to be skeletons of E_mW_n. This skeleton part could survive the fragmentation, although some of the ethanol molecule(s) can be evaporated. The dominance of the ethanol polymers in the mixture may have originated in a structure-broken aqueous environment. For stabilizing structured clusters, it is necessary to have a flexible medium that surrounds the rigid clusters. The intensity of the 2.8 Å peak in the RDFs in Fig. 6 drastically decreases with increasing x_E. Even at $x_E = 0.4$, the 2.8 Å component is approximately 30% of that of pure water. This is consistent with the mass spectra of this solution, where pure water clusters are missing and the average hydration numbers (N^a) are smaller than m at $x_E > 0.2$, as shown in Fig. 4. In this region, the greater part of water molecules does not form linear hydrogen bonds with the average O–O distance of 2.8 Å. They may exist just as filler molecules.

With the aid of filler water molecules, ethanols could form polymer structures in the mixture. For the closest parallel configuration of two ethyl groups in an ethanol polymer, one can select the fundamental conformations of the polymer chain. Figure 7 shows the two conformations of an ethanol trimer: *syn-syn* conformation where the three ethyl groups are located on the same plane, and an *anti-anti* conformation where the ethyl groups are located to the back plane and the front plane alternatively. In both cases, the closest methylene–methylene and methyl–methyl distances are commonly 4.6 Å for a hydrogen bond distance of 2.8 Å. The *anti-anti* conformation requires more volume and the hydrating water molecules are separated from each other. On the other hand, the *syn-syn* conformation allows the hydrated water molecules to be hydrogen-bonded

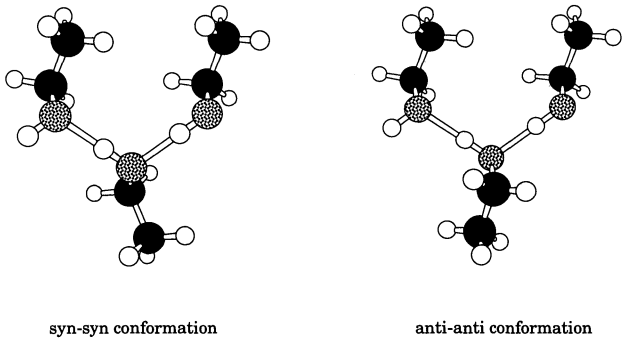

Fig. 7. Two conformers of ethanol trimer with parallel orientation of ethyl groups.

to each other, resulting in a total binding energy that is much larger than that for hydrated clusters in the *anti-anti* conformation. Thus, the *syn-syn* conformation is energetically more favorable than the *anti-anti* conformation for hydrate cluster formation. However, for smaller clusters ($m < 8$), the *anti-anti* conformation must also be stable, since the lower ethanol clusters are hardly hydrated (Fig. 1).

In a solution at room temperature the hydrogen bonds are expected to be dissociated and created on a time scale much shorter than 100 ns.[30,31] However, as long as the two molecules are located adjacently, the dissociated hydrogen bond(s) can ben recreated due to the attractive interaction. Important is the cooperative intermolecular motions of the associated molecular groups. The motion of massive and bulky molecules associated with each other is a quite an important factor concerning the lifetimes of the clusters. The hydrogen bonds between less mobile molecules (ethanol molecules in this case because of its mass (46) larger than that of water molecules (18)) can be seen for a longer time than those of small molecules. The separation of an ethanol–ethanol pair to a sufficiently long distance may take a much longer time than that of a water–water pair or an ethanol–water pair. This situation favors larger ethanol polymers with their longer lifetimes. The evolution of pure ethanol clusters might be elucidated with such simple mechanics. A molecular dynamics calculation on the ethanol–water mixture system will be highly helpful for examining the preferability of ethanol chain formation to ethanol–water mixed cluster formation. The success of the hydration number analysis with simple Poisson distribution functions for ethanol polymer hydrates demonstrates that the hydration number is a function of the ethanol polymer size (m). The observed average hydration numbers (N^a) in the $0.2 \leq x_E \leq 0.8$ region is expressed by Eq. 8. The form of this equation provides us with very important clues concerning the structure of the polymer hydrates. Firstly, the basic structure of the polymer hydrates must be common in $0.2 \leq x_E \leq 0.8$. Secondly, N^a is a quadratic function of the polymer size (m). This indicates the possibility that the evolution of the hydrate species involves the

evolution of two ethanol polymers simultaneously. In other words, the water molecules are shared with two ethanol polymers or the two parts of one ethanol polymer. Thirdly, although we have no possibility of having any polymer hydrate at $x_w=0$, the hydrates have a fundamental structure that is independent of the water concentration.

On the basis of the above discussion as well as the radial distribution functions given in Fig. 6, we propose a model structure that can explain all of the observed results in the present study. The basic structure is shown in Fig. 8. This cluster has two ethanol polymer units with a *syn-syn* ethanol orientation. In each ethanol polymer unit, ethyl groups are located on the same plane. On the inner side of the two planes, the ethanol oxygen groups are facing each other with bridging water molecules. By fixing all of the hydrogen-bonding O–O distances to be 2.8 Å, one can obtain a distance of 7.0 Å between the two ethyl planes. In fact, the RDF of the $x_E=0.2$ solution in Fig. 6 shows a peak at 7.0 Å. This peak gradually decreases with increasing x_E. This sandwitch-type structure requires

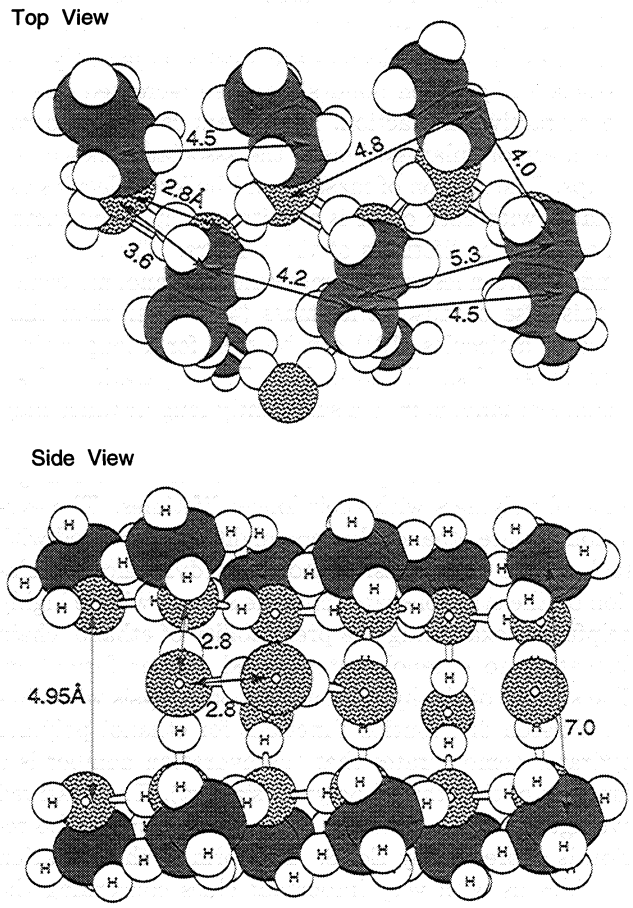

Fig. 8. A model of an ethanol polymer-hydrate constructed based on the mass spectral analysis and RDFs of ethanol–water mixtures with $0.2\leq x_E\leq 0.4$. The distances were derived by fixing all of the hydrogen bonds to be 2.8 Å.

the presence of bridging (or spacing) water molecules. Therefore, the appearance of the x_w free part in Eq. 8 is elucidated by introducing at least two bridging water molecules to form one hydrate cluster. With increasing x_w, water molecules will occupy not only the bridging sites, but also the lone pair sites of the bridging water molecules (see Fig. 8). This kind of water molecule is called a parallel water molecule, which differs from the bridging water molecules; it is shown in the bottom of the top view and in the middle left of the side view of Fig. 8. The parallel and perpendicular bridging water molecules form an intermediate water layer between the two hydrophobic layers. The interatomic distances obtained by fixing all hydrogen-bonding O–O distances at 2.8 Å are also shown in Fig. 8. The RDF for the solution at $x_E=0.2$ showed a second broad peak at 4.2—4.8 Å. This peak may contain the carbon–carbon distances of the nearest two ethyl groups in the polymer, which are estimated to be ca. 4.6 Å in the model.

At a higher ethanol concentration, the bridging water molecules are prone to be lost and the two ethanol polymer planes are in contact with each other. However, the OH groups of the each polymers do not necessarily face each other any more, but suffer from repulsive forces between the oxygen atoms as long as the ethanol polymer chains are maintained in the original planes. The rotational activity induced by the repulsion may dissociate the original hydrogen bonds in the planes, and allow the formation of new hydrogen bonds along the perpendicular direction. The average ethyl–ethyl distance in the plane will be slightly elongated. The strongest interatomic peak at 4.8 Å observed for a pure ethanol solution (top of Fig. 6) is thus attributed to the carbon–carbon distance of the neighboring two ethanols located in parallel. The weaker, but clear, peaks at 3.8 and 4.3 Å in the pure ethanol solution are also attributed to the C–O and the C–C distances of the two ethanols directly bonded while facing each other, respectively.

Conclusions

Ethanol–water mixtures showed a distinctive feature of ethanol polymer formation. No cluster characteristic of an aqueous solution was observed at $x_E\geq 0.2$, while ethanol polymers and their hydrate clusters are dominant species found in the $0.2\leq x_E\leq 0.8$ region. The concentration dependence of RDF and the mass spectra indicated that most water molecules are not bonded to each other, but may exist just as stabilizers for ethanol polymer (hydrate) clusters. The model of ethanol polymer hydrates presented above explains the observed results.

This work was supported by a Grant-in-Aid for Scientific Research (A) No. 04403002 and for New Program "Intelligent Molecular System with Controlled Functionality" No. 06NP0301 from the Ministry of Educa-

tion, Science and Culture. We thank Messrs. M. Ihara and H. Ohzono for their technical assistance in the X-ray diffraction measurements.

References

1) A. G. Mitchell and W. F. K. Wynne-Jones, *Discuss. Fraday Soc.*, **15**, 161 (1953).
2) K. Nakanishi, *Bull. Chem. Soc. Jpn.*, **33**, 793 (1959).
3) F. Franks and H. H. Johnson, *Trans. Fraday Soc.*, **58**, 656 (1962).
4) F. Franks and D. J. G. Ives, *Q. Rev., Chem. Soc.*, **20**, 1 (1966).
5) A. Ben-Naim, *J. Chem. Phys.*, **67**, 4884 (1977).
6) H. H. Ruterjans and H. H. Scheraga, *J. Chem. Phys.*, **45**, 3296 (1966).
7) A. Coccia, P. L. Inodovia, F. Podo, and V. Viti, *Chem. Phys.*, **7**, 30 (1975).
8) S. Mashimo and T. Umehara, *J. Chem. Phys.*, **95**, 6257 (1991).
9) A. H. Narten and H. A. Levy, *J. Chem. Phys.*, **55**, 2263 (1971).
10) R. Carban and M. D. Zeidler, *Ber. Bunsenges. Phys. Chem.*, **96**, 1463 (1992).
11) A. V. Okhulkov, Yu. N. Demianets, and Yu. E. Gorbaty, *J. Chem. Phys.*, **100**, 1578 (1994).
12) W. H. Zachariasen, *J. Chem. Phys.*, **3**, 158 (1935).
13) G. G. Harvey, *J. Chem. Phys.*, **7**, 878 (1939).
14) A. K. Soper and J. L. Finney, *Phys. Rev. Lett.*, **71**, 4346 (1993).
15) J. L. Finney and A. K. Soper, *Chem. Soc. Rev.*, **1994**, 1.
16) A. H. Narten and A. Habenschuss, *J. Chem. Phys.*, **80**, 3387 (1984).
17) K. Nishikawa and T. Iijima, *J. Phys. Chem.*, **97**, 10824 (1993).
18) N. Nishi, S. Takahashi, M. Matsumoto, A. Tanaka, K. Muraya, T. Takamuku, and T. Yamaguchi, *J. Phys. Chem.*, **99**, 462 (1995).
19) N. Nishi, K. Koga, C. Ohshima, K. Yamamoto, U. Nagashima, and K. Nagami, *J. Am. Chem. Soc.*, **110**, 5264 (1988).
20) N. Nishi, *Z. Phys. D: -Atom, Molecules and Clusters*, **15**, 239 (1990).
21) K. Yamamoto and N. Nishi, *J. Am. Chem. Soc.*, **112**, 549 (1990).
22) K. Yamanaka, T. Yamaguchi, and H. Wakita, *J. Chem. Phys.*, **101**, 9830 (1994).
23) M. Ihara, T. Yamaguchi, H. Wakita, and T. Matsumoto, *Adv. X-Ray Anal. Jpn.*, **25**, 49 (1994).
24) G. Johansson and M. Sandström, *Chem. Scr.*, **4**, 195 (1973).
25) "International Tables for X- Ray Crystalloghy," Kyonoch Press, Birmingham (1974), Vol. 4.
26) T. Takamuku, T. Yamaguchi, and H. Wakita, *J. Phys. Chem.*, **95**, 10098 (1991).
27) A. J. Stace and A. K. Shukla, *J. Am. Chem. Soc.*, **104**, 5314 (1982).
28) Y. Tanaka, N. Ohtomo, and K. Arakawa, *Bull. Chem. Soc. Jpn.*, **57**, 2369 (1984).
29) K. Yamamoto and N. Nishi, *J. Am. Chem. Soc.*, **112**, 549 (1990).
30) H. Tanaka and I. Ohmine, *J. Chem. Phys.*, **87**, 6128 (1987).
31) M. Sasai, I. Ohmine, and R. Ramaswamy, *J. Chem. Phys.*, **96**, 3045 (1992).